Journal of Organometallic Chemistry, 235 (1982) 383—393
Elsevier Sequoia S.A., Lausanne — Printed in The Netherlands

A THEORETICAL STUDY OF THE ELIMINATION PROCESS OF METHANE FROM A PLATINUM COMPLEX

A. FLORES—RIVEROS

Instituto Mexicano del Petróleo, Eje Central Lázaro Cárdenas 152, Apdo. Postal 14-805, 07730 México, D.F. (México)

and O. NOVARO *

Instituto de Física, Universidad Nacional Autónoma de México, Apdo. Postal 20-364, Delegación Alvaro Obregón, 01000 (México)

(Received November 9th, 1981; in revised form February 23rd, 1982)

Summary

A theoretical analysis of the dissociative reaction *cis*-$PtH(CH_3)(PX_3)_2 \rightarrow Pt(PX_3)_2 + CH_4$ is presented. Several aspects of the effect on the mechanism of this reductive elimination when the substituent X is changed ($X_3 = (CH_3)_3$, case I and $X_3 = CH_2Cl(CH_3)_2$, case II), are considered and compared with the corresponding experimental facts. This indicates the following: the kinetic barrier for case I is small and even if a concerted mechanism is implied, an almost spontaneous process is strongly indicated. The activation energy is lowered in case II, where the presence of an electronegative substituent makes even easier the performance of a spontaneous process. The study of the reaction pathway was carried out through an Extended Hückel calculation.

1. Introduction

The hydrogenation of alkenes catalyzed by organometallic complexes, very often implies the formation of *cis*-hydridoalkylmetal complexes during some intermediate stages of the process. Thus intramolecular reductive elimination of the alkane is assumed to occur during such reactions [1]. Recently, the synthesis and characterization of *cis*-hydridoalkylphosphineplatinum compounds have been reported [2]. In ref. 2 the kinetics of the reaction gave evidence for an intramolecular reductive elimination of the alkane product, as follows:

cis-$PtH(CH_3)(PX_3)_2 \rightarrow Pt(PX_3)_2 + CH_4$ (1)

* Consultant at Instituto Mexicano del Petróleo.

0022-328X/82/0000—0000/$02.75

where the X moieties were *para*-substituted phenyl groups. These groups showed a notable influence on the kinetics and thermodynamics of the process.

A recent theoretical work [3] fairly agrees with such experimental results, albeit referring to other metals. An ab initio study [4] of the $Ni(CH_3)_2(H_2O)_2$ system suggests that the same tendencies are present in similar organometallic complexes. In addition, an important theoretical analysis [5] has been carried out providing the symmetry requirements for reductive elimination regarding the concerted reactions:

$$R_2ML_n \rightarrow R{-}R + ML_n$$

in which the forbidden and allowed processes, depending upon the *d*-orbital spin state of the metal, are discussed.

In the present paper we shall report a study of the process kinetically characterized in ref. 2, based on a molecular orbital analysis of the organometallic complex. In the following section we discuss the structure chosen for this complex and its evolution during the reductive elimination reaction plus some details of the calculational method used. In section 3 the results concerning the energy changes and wave functions for the system are used to describe the reaction pathway and to derive the bond orders and the nature of the molecular orbitals. Finally, there is a section devoted to the discussion of these results and their application to the understanding of the process.

2. Theoretical method and model

The method used here for the molecular orbital study of the elimination process is based on the Extended Hückel approximation. This method has been thoroughly discussed in the literature [6] and the parameters necessary for the present calculations are the same reported by Thorn and Hoffmann [7]. The method and parameters appear in Appendices A and B. The geometry of the complex and the movements that the moieties undergo during the intramolecular reaction of eq. 1 are depicted in Fig. 1. The geometrical parameters that describe these movements comprise: the angle between the reacting groups (φ); the separation from the metal to the methyl (R); the angle between the phosphines (θ); the separation from the metal to the H (r) and the rocking angle between the local three-fold axis of the methyl group and the extension of the axis of the Pt—CH_3 bond (α). A more complete geometrical optimization would of course be desirable, but it is beyond our means since it represents the optimization of all of the degrees of freedom of the system. Furthermore, it is generally accepted from the experimental data [2] that the reaction pathway mainly consists of the concerted variation of θ and φ (see Fig. 2). Thus we optimized the initial structure for case I, i.e. the complex $PtH(CH_3)(P(CH_3)_3)_2$ and then followed an optimal pathway leading to the linear complex $Pt(P(CH_3)_3)_2$ and a released methane, as represented in Fig. 2. Such a trajectory was assumed to be the same for case II in order to allow for a consistent comparison between both cases, as shall be discussed below.

For convenience the reaction pathway was divided in six successive steps starting from step 0 (the initial configuration of the complex). The geometrical changes in the relevant parameters for each of these steps are reported in Table

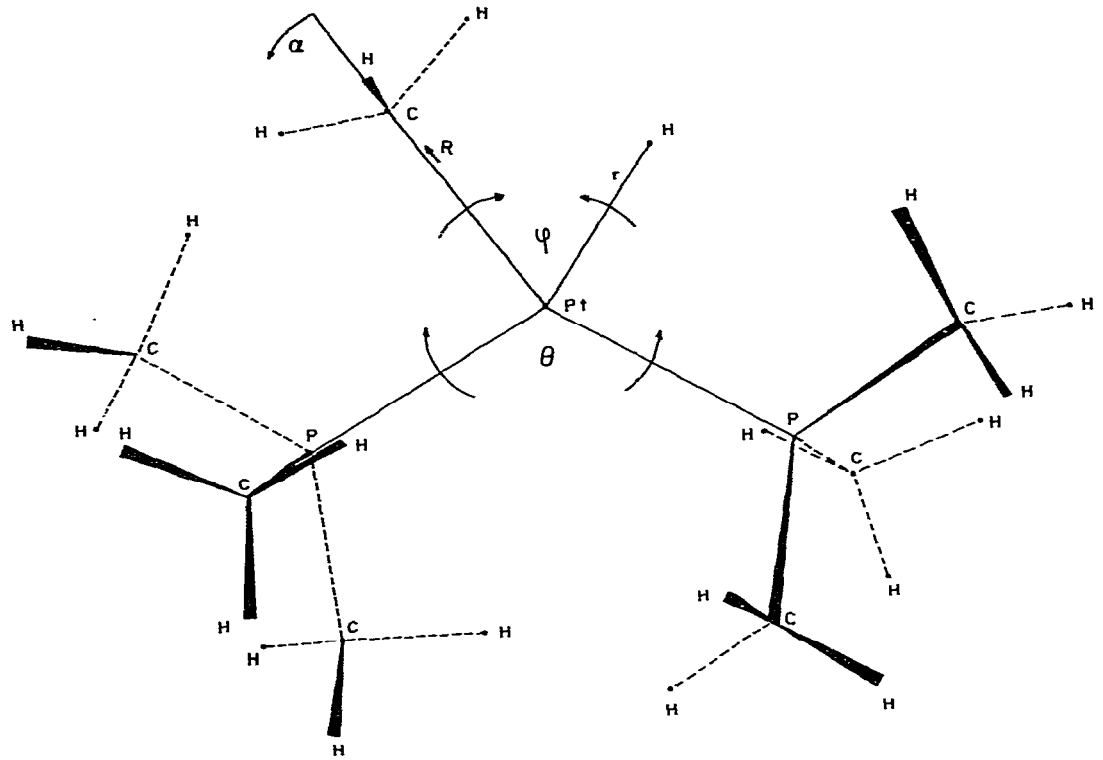

Fig. 1. Scheme of the $PtH(CH_3)(PX_3)_2$ complex, showing the degrees of freedom associated to the proposed geometrical movements.

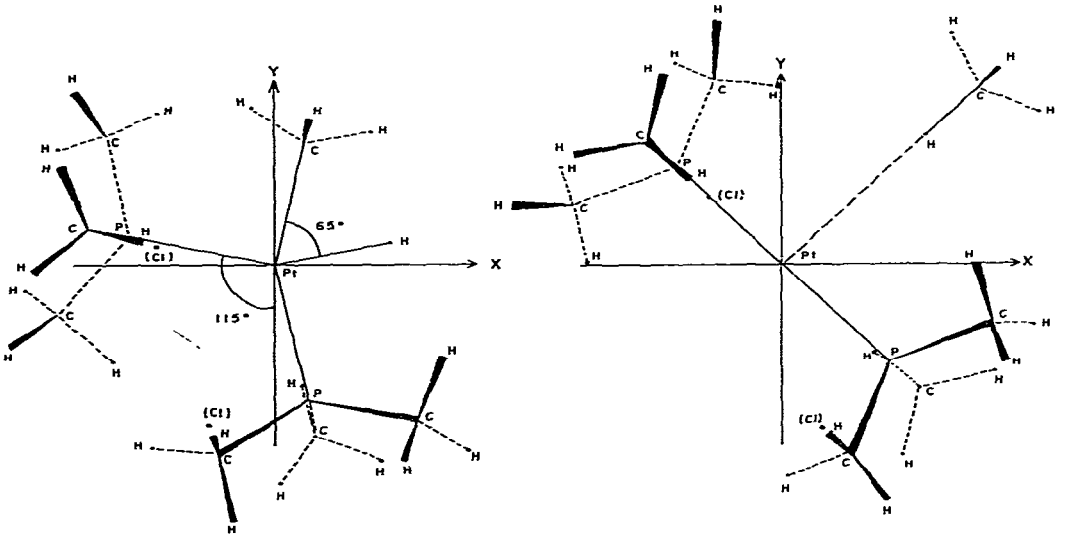

Fig. 2. Representation of the initial and final steps of the process. The former shows the coordinated complex and the latter illustrates the products obtained through the reductive elimination. The (Cl) represent the positions where chlorines replace the hydrogens in Case II.

TABLE 1

VARIATION OF THE GEOMETRICAL PARAMETERS THROUGHOUT THE REACTION

Lengths are given in Å

	In	1	2	3	4	5	Fin.
θ	115°	128°	141°	154°	167°	180°	180°
φ	65°	52°	39°	26°	13°	7°	0°
R	2.10	2.24	2.37	2.51	2.64	2.78	4.11
r	1.7	1.7	1.7	1.7	1.7	1.7	3.0
α	0°	2°	4°	6°	8°	10°	0°

1, Steps 0 and 7, called Initial and Final in Table 1, correspond to the geometries represented in Fig. 2.

3. Results

We now shall proceed to present the results of the calculations by discussing, first, the evolution of the energies, the most relevant information given by any quantum mechanical calculation and then the overlap populations as well as the characterization of the molecular orbitals, to further supplement this information.

a. Energy of the system

In Fig. 3 we represent the evolution of the energy during the reductive elimination reaction of eq. 1, for case I (i.e. $X_3 = (CH_3)_3$). The energy is plotted as a function of the seven steps discussed in section 2 and defined in Table 1. For this case, where all of the three phosphine substituents are simply CH_3 groups, it is seen that the reaction coordinate implies the surmountal of a relatively small activation barrier (25 kcal/mol). Furthermore the evident final stabilization implies an exothermic process, yielding over 50 kcal/mol. Thus the Extended Hückel results lead to the prediction of a kinetically feasible reaction and also to a thermodynamically facile reaction, while in contrast, the reverse process would present a strong thermodynamical impediment. All these results fit extremely well the experimental data of the process [2], as shall be discussed in section 4. In Fig. 4 the corresponding energy evolution for case II is reported. We remind that case II differs from case I in the substitution of one of the methyls pertaining to the phosphines by a CH_2Cl group. The reason for this choice was based on the experimental results of ref. 2, where it was shown that

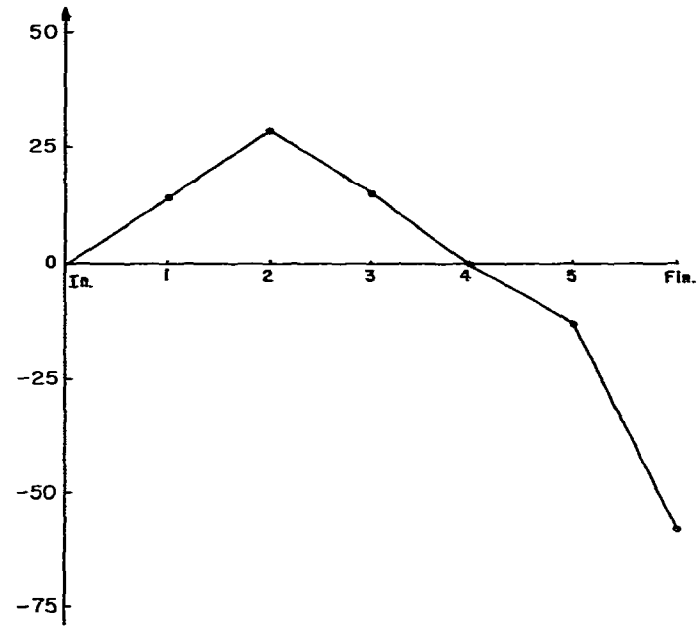

Fig. 3. Energy evolution for Case I: $X_3 = (CH_3)_3$, as a function of the reaction steps. Units are given in kcal/mol.

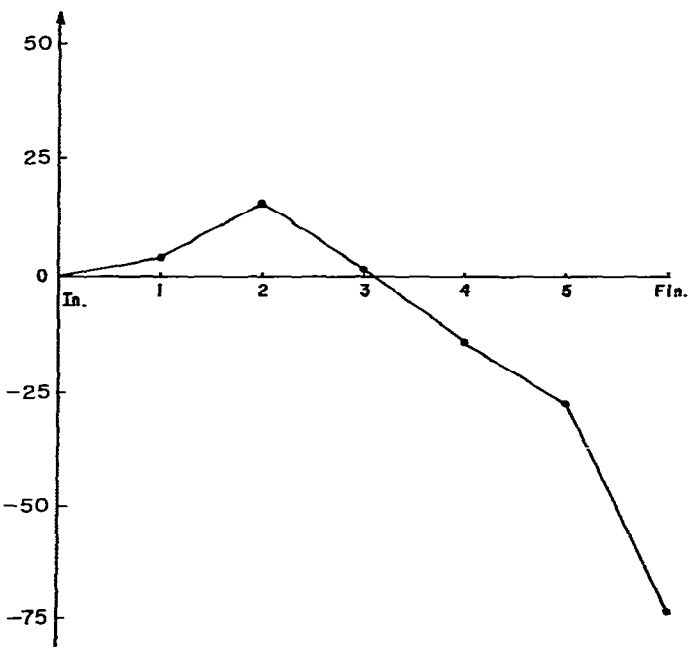

Fig. 4. Energy evolution for Case II: $X_3 = (CH_2Cl)(CH_3)_2$. Units are given in kcal/mol.

electron withdrawing substituents in the phosphine (notably Cl) increases the driving force of the reaction. Although in ref. 2 phenyl groups were used for X while we used methyls, we believe that our cases I and II should model this effect (this type of representation of larger hydrocarbons by smaller ones is, on the other hand, quite common in this type of theoretical studies [7,8]).

Figure 4 shows, in effect, that a more electronegative substituent does indeed imply an apparent lowering of the barrier (surmounting 14 kcal/mol), as expected. The mechanism becomes also an essentially spontaneous process. Again, in section 4 we shall relate this effect to the results of ref. 2.

It is also interesting in Fig. 4 that the exothermicity of the process appears to be even larger in case II (in fact, over 63 kcal/mol).

It should be mentioned that the initial configuration was optimized for case I, and then also used for case II in order to properly compare between them. However, we must remark that within the same configuration the Cl position in the substituted methyl groups was very carefully chosen, to avoid the possibility of spurious steric repulsion effects.

b. Overlap population

The evolution of the reaction is more easily visualized by looking at the overlap populations as given in Fig. 5. Only the most relevant bonds during the process are reported, as they change in the sequence of seven steps, both for cases I and II. A comparatively smooth change in these overlap populations is evident, with the Pt—H and Pt—CH_3 bonds gradually breaking (especially the latter due to the rapid depopulation of the Pt—CH_3 overlap) and the formation of a new

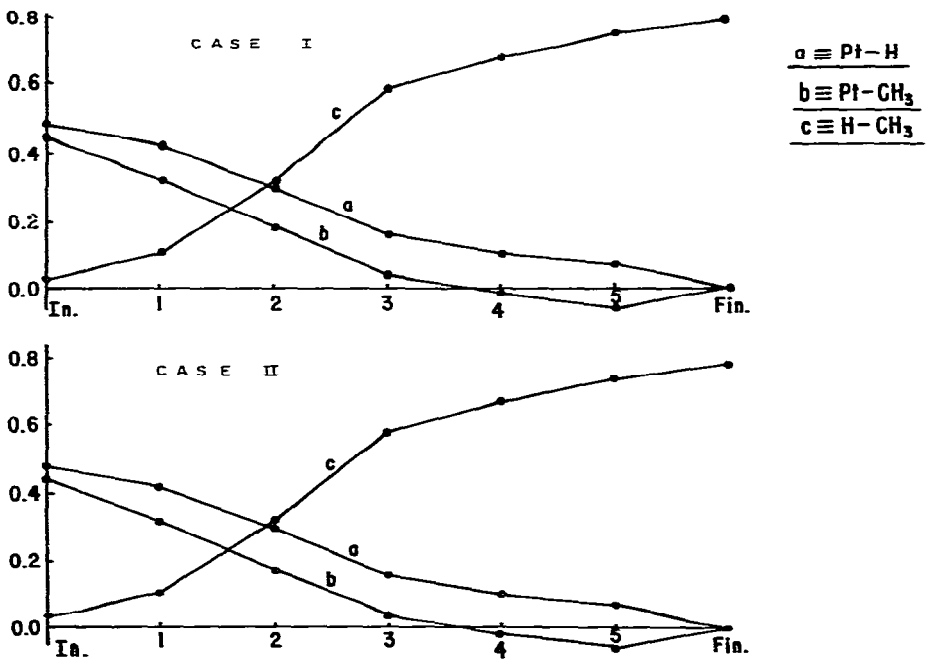

Fig. 5. Overlap population for the relevant bonds as a function of the reaction stages, shown for both cases.

C—H bond between the methyl and hydrogen moieties originally coordinated with the metal. Step 2 evidently corresponds to a transition state where the new bond replaces the old ones. Interestingly for both cases step 2 is precisely the top of the activation barrier, and when the system surmounts it, the energy monotonically goes down (see Fig. 3). The parallel behaviour between both cases points out undoubtedly to the same chemical image.

c. Molecular orbital analysis

The reductive elimination takes place from a *cis*-tetracoordinated complex of the type

$$d^8\text{-MRR'L}_2 \rightarrow d^{10}\text{-ML}_2 + \text{RR'}.$$

Such type of reactions are inherently of low symmetry [9]. In the present study this indeed occurs from the initial step and is enhanced during the subsequent geometrical movements, resembling rather an alkyl insertion mechanism. Therefore, the system does not allow the classification of the orbital energy levels, but rather the establishment of each of the atomic orbital contributions associated with the relevant bonds Pt—CH_3, Pt—H and CH_3—H throughout the reaction. In Fig. 6 we depict such atomic orbital participation, in the manner of an energy correlation diagram, illustrating only the initial and final steps.

Figure 6 depicts some of the highest occupied molecular orbitals of the

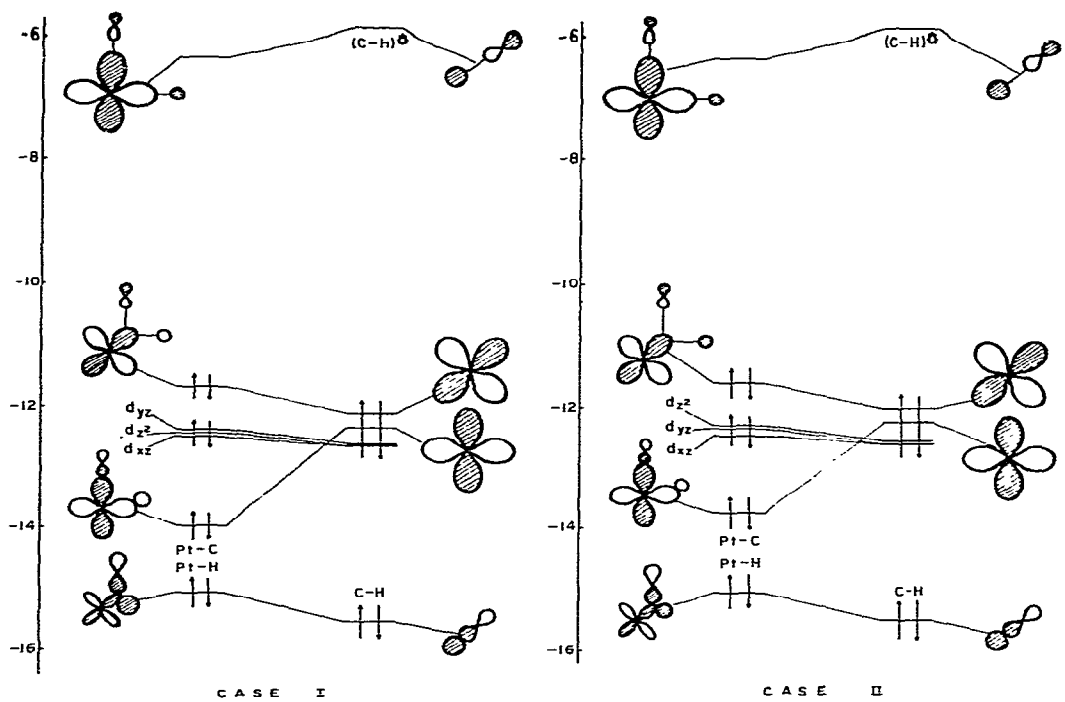

Fig. 6. Correlation diagram illustrating the molecular orbital contributions associated with the elimination of methane, shown for both cases. Only the initial and final steps of the process are represented. Orbital energies are given in eV.

complex plus a single virtual orbital (the lowest unoccupied molecular orbital LUMO). The latter is not very relevant to the process, being at the beginning of the reaction an antibonding orbital between the metal atom and the reacting moieties and at the end antibonding between these moieties themselves. The occupied states represented in Fig. 6 are mostly related to the Pt *d*-states. Among these the d_{z^2}, d_{xz} and d_{yz}, i.e. the metal atom orbitals not directly related to the reaction plane (xy) evolve as expected, remaining virtually unchanged throughout the reaction, for both cases. The d_{xy} orbitals are essentially concentrated in the highest occupied molecular orbital (HOMO) in both cases. It is notable that this HOMO is *antibonding* with respect to the CH_3 and H groups. In other studies of organometallic complexes the HOMO is usually [10,11] associated to the most labile bonds of the organometallic complexes, either giving an antibonding [10] or bonding [11] contribution to these bonds. For the second type of complexes, the lability comes from the possibility of thermal depopulation of the HOMO, thus labilizing the bond it represents [11] while for the first type, which is the one that applies to the present study, the weakness of the bonds is even greater, because the antibonding state is doubly occupied in the initial complex. For such complexes, energy barriers are small [10].

The d_{xy} character is also slightly manifested by one of the lower orbitals where it is *bonding* towards the CH_3 and H groups. Thus at the initial stages the metal d_{xy} state is acting as an agent for the bonding between these reacting moieties. At the end, of course, the d_{xy} participation on this molecular orbital is gone and the latter becomes the new C—H bond.

The main difference between our cases I and II in Fig. 6 is the evolution of the $d_{x^2-y^2}$ orbital which is bonding to the CH_3 and H groups. For both cases this molecular orbital is noticeably *destabilized* towards the end of the process, but somewhat less in case II. Actually, for the latter case the molecular orbital energy difference is 0.12 eV smaller than for case I.

We conclude that the energy increase of the $d_{x^2-y^2}$ orbital, which implies a destabilization, is related to the activation barriers and therefore it explains why this barrier is lower in case II, in which this energy increase is also smaller. This is in accordance with the conclusions of Tatsumi et al. [3] who among other findings report the notable participation of the *d*-orbital levels of Ni and of Pd (notably a d_{xy} destabilization which due to their choice of coordinates plays a similar role as our $d_{x^2-y^2}$ orbital).

We can summarize the present discussion noting that the facility of the reductive reaction is reflected in the low-lying antibonding orbitals for the metal—reactants bonds (they are the HOMO and LUMO of Fig. 6). Furthermore, the electronic effect caused by the chlorine substitution is then interpreted in a natural manner at a molecular orbital level.

4. Conclusions

The main conclusion derived from the results of the preceding section is essentially that the reductive intramolecular reaction appears to be not only feasible but in fact facile, due to the smallness of the energy barrier for both cases. This is in excellent agreement with the experimental data [2] on this

system, which is one of the first cases where such simple intramolecular reductive eliminations have been observed and kinetically characterized. Furthermore the fact that it proceeds even at quite low temperatures has led Abis et al. [2] to conclude that the energy barrier is small, and if electron-withdrawing substituents (particularly Cl) are included in the phosphine ligands the reaction rate increases quite notably. This again is well described by the present calculations where the inclusion of Cl substituents relaxes the kinetic impediment for the reaction, in case II.

For both cases a very important stabilization of the energy towards the valley of the products is evidenced in Fig. 3 and 4, providing a justification of the assumption [2] that the reverse reaction (oxidative addition of methane) is not feasible due to thermodynamic rather than kinetic considerations.

It also should be mentioned that a recent paper [3] using the same theoretical method reached among others, the following conclusions: the activation energy is enhanced by having stronger donor ligands *trans* to the reacting groups and by the electron donation from the latters towards the metal complex. Furthermore, the barrier in tetracoordinated complexes, such as the one studied here, was found to be controlled by the energy of the metal levels, notably the antisymmetric d_{xy} orbital [3]. Not only is the latter result evident in the molecular orbital analysis of the preceding section, but in the closely parallel substituent effects in both studies. Evidently if electron donation by the *trans*-groups would augment the barrier an electron-withdrawing Cl would be expected to have an opposite effect, as we have obtained. This excellent agreement is not surprising because in both cases the same quantum mechanical model was utilized, but the equally good agreement found with the experimental conclusions of Abis et al. [2] gives confidence that the Extended Hückel approximation can represent adequately these processes, at least as concerns the present study.

Acknowledgments

We want to express our gratitude to Prof. Roald Hoffmann not only for providing us with the Extended Hückel program and for making available to us several preprints of this group, but also for his extremely kind interest and assistance. One of us (A.F.) acknowledges the hospitality of Cornell University during a short visit. We are also grateful to Dr. Marisa Ruiz for her interest and help along this work as well as to the IBM computing department at the Instituto Mexicano del Petróleo.

This work was supported in part by CONACYT through project PCCBNAL 790438.

Appendix A

The method used here is the Extended Hückel theory developed by Hoffmann [6], based on the expansion of the molecular orbitals of the system into a linear combination of atomic orbitals:

$$\Psi_i = \sum_j C_{ij} \phi_j$$

These wave functions are then used to optimize a Hückel-type Hamiltonian, free of the assumption of zero differential overlap. This yields, on minimization of the total energy, the set of Hückel equations:

$$\sum_{i=1}^{n} \{H_{ij} - E S_{ij}\} C_{ij} = 0 \qquad j = 1, 2, ..., n$$

This method is particularly adequate for conformational predictions, charge distributions, etc. Of course it is limited in several aspects such as spectral predictions and also needs a careful choice of parameters, especially in its recent extension to organometallic molecules [3].

Appendix B

The parameters of the Extended Hückel calculation are listed in Table 2. A "weighted H_{ij}" formula was used [12]. The H_{ii} values, the Pt 5*d*, C 2*s* and 2*p*, H 1*s*, Cl 3*s* and 3*p* were taken from ref. 7, while those of Pt 5*d*, P 3*s* and 3*p* were from ref. 13.

TABLE 2

PARAMETERS OF THE EXTENDED HÜCKEL CALCULATION

The Orbital energies, H_{ii}, are given in eV

ATOM	ORBITAL	H_{ii}	ORBITAL EXPONENT ✡
Pt	6 s	−9.077	2.554
	6 p	−5.475	2.535
	5 d	−12.59	6.013 (0.6334) 2.696 (0.5513)
P	3 s	−18.6	1.75
	3 p	−14.0	1.30
C	2 s	−21.4	1.625
	2 p	−11.4	1.625
H	1 s	−13.6	1.30
Cl	3s	−30.0	2.033
	3p	−15.0	2.033

✡ For the d functions a double zeta expansion was used. The expansion coefficients are given in parenthesis.

Geometrical assumptions included the following: Pt—C 2.1, Pt—H 1.7, Pt—P 2.3, P—C 1.82, C—H 1.11 and C—Cl 1.76 Å, $P(CH_3)_3$, $P(CH_2Cl)(CH_3)_2$, CH_3 and CH_2Cl systems were assumed tetrahedral.

References

1 B.R. James, Homogeneous Hydrogenation, Wiley, New York 1973.
2 L. Abis, A. Sen and J. Halpern, J. Am. Chem. Soc., 100 (1978) 2915.
3 K. Tatsumi, R. Hoffmann, A. Yamamoto and J.K. Stille, Bull. Chem. Soc. Japan 54 (1981) 1857.
4 B. Akermark, H. Johansen, B. Roos and U. Wahlgren, J. Am. Chem. Soc., 101 (1979) 5876.
5 B. Akermark and A. Ljungquist, J. Organometal. Chem., 182 (1979) 59.
6 R. Hoffmann, J. Chem. Phys., 39 (1963) 1397.
7 D.L. Thorn and R. Hoffmann, J. Am. Chem. Soc., 100 (1978) 2079.
8 J.G. Norman, Inorg. Chem., 16 (1977) 1328.
9 R.G. Pearson, J. Am. Chem. Soc., 94 (1972) 8287.
10 O. Novaro, S. Chow and Ph. Magnouat, J. Catal., 41 (1976) 91.
11 O. Novaro, E. Blaisten—Barojas, E. Clementi, G. Giunchi and M.E. Ruíz—Vizcaya., J. Chem. Phys., 68 (1978) 2337.
12 J.H. Ammeter, H.B. Burgi, J.C. Thibeault and R. Hoffmann, J. Am. Chem. Soc., 100 (1978) 3686.
13 H. Basch and H.B. Gray, Theoret. Chim. Acta (Berl.), 4 (1967) 367. Such parameters are also specified in a manual corresponding to a recent version of the Extended Hückel program, and kindly supplied to us by Prof. Roald Hoffmann.